

Effect of Amorphous Layer on the Microstructure and Properties of Al-B₄C Layered Composite

Paulo A. Inacio^{*1}, Yubo Zhang^{*#2}, Jinchuan.Jie^{*3}, Tingju. Li^{*4}

^{*}Key Laboratory of Solidification Control and Digital Preparation Technology (Liaoning Province), School of Materials Science and Engineering, Dalian University of Technology, Dalian 116024, China

[#]State Key Laboratory of Metal Material for Marine Equipment and Application, Anshan, 114000, China

Abstract - An Al-Al+B₄C-Al layered composite was produced by semi-continuous casting and hot rolling method, the innerlayer is Almatrix reinforced by 40wt.% B₄C (F60), while the outlayer is pure Al. The result shows that the composite innerlayer (Al-B₄C) has a high macrohardness of 43HBS1.5/125/30, once the outlayer pure Al has 16.5HBS1.5/125/30. However, due to the significant difference between Al and B₄C in the inner layer, there are always defects near their interface and there is a sharp hardness gradient. By means of surface alloying, oxidation and acid attack on the reinforcement surface, a microamorphous transition (MAT) layer was found bounding the reinforcement's particles. The microhardness behaviour shows the MATlayer has ~900HV (1Kg/15s) on the reinforcement boundary and decays exponentially until the transition layer have no effect on the Almatrix (~32HV). This MAT layer bounding the reinforcement reduces the properties gradient and raises the composability, leading to a better impact resistance.

Keywords: B₄C, layered composite, Amorphous Layer, Reinforcementtreatment.

I. INTRODUCTION

Aluminum metal matrix composites (AlMMC also called AMC) consists of at least one metal and a reinforcement material, such as fiber, particles, compounds, oxides, carbide etc., in order to achieve the requirements and expected properties which cannot be met by single compound materials [1]-[4]. Though designing an optimized structure, AMC can achieve better performance. For example, by mixing Alalloy and B₄C powers together we can obtain a light and hard composite. Boron carbide (B₄C) has a high melting point, outstanding hardness, good mechanical properties, low specific weight, and great resistance to chemicals [5]-[12]. On the other hand, Al alloys have low density, low cost, and good properties [13].

A threelayered (soft-hard-soft) composite is proposed to take full advantage of each material, consisting of pure Al outlayers and a B₄C reinforcement Almatrix as core (inner layer). Such composite can combine the core high hardness

of B₄C particlereinforced and the outer layer weldability and toughness.

Composites with reinforcementssize up to 100 mesh and high wt.% are desired to shielding and protective armour applications, also has applications as abrasive material and proton absorption. However, the addition of large size reinforcements also introduces some defects, such as brittleness elevation, high unbound ratio and big properties gradient on reinforcementmatrix interface [13]-[14]. In addition, the recommended balance of the ceramic reinforcements in AMCs is less than 20 wt.%, when this value is exceeded the AMC significantly increases their brittleness, but by reducing the reinforcement content it reduces the hardness range and it no longer meets the high hardness requirements. Thus, a lot of work is needed to manufacture a worthwhileAMC with large reinforcement size and high wt.%, simultaneously.

In general, many routes can produce AMC; one of those is the powder metallurgy (PM) by blending elemental or prealloyed powders together. However, it is uneconomical to industrial production and the products of metallurgy can have limited shapes and features, which limit its wide application. On the other hand, the casting method can achieve efficient production and low cost. However, some problems as particle agglomeration and low interface interaction between B₄C and Al need to be resolved[14]. In our previous study, a semi-continuous casting followed by a hot rolling process were designed to fabricate a threelayered composite material consisting of an Al outer layer and a 7075-B₄C inner layer.

In the present work, by means of metal addition, oxidation and surface acid attack (SAA) a microamorphous transition (MAT) layer was made bounding the surface of B₄C (F60) in order to counter large size and high content disadvantages such as: high gradient properties between the hard reinforcement and ductile matrix, reinforcement surface defects and low Al-B₄C interface reactivity. Optimizing those parameters on the innerlayer, the final composite macro properties as hardness and toughness rises allowing their utilization in composites innerlayer [15]-[17].

II. EXPERIMENTAL PROCEDURES

For the final composite acquisition, two main steps are required:

A. Reinforcement treatment

The first step aims to oxidize the reinforcement surface flaws and inlay some substrate to promote the formation of the MAT layer. The nickel has high interface affinity with B_4C and Al as was investigated [18]-[20], leading to the utilization of this metal. The amount of 5wt.% thin Ni(99.99%) is mixed with B_4C , the powder is placed into a rotary drum mixer at 3.14 rad/s for 120 min. The peak of oxidation in humid air that doesn't compromise the whole reinforcement properties is deeply investigated [10]-[11], [21]-[23] and a common denominator is found around 1173K and 120 minutes.

The B_4C powder nominal size of 60 mesh is used, the size distribution of which is a compound normal distribution, i.e., the size of 90% the B_4C is in the range of 250-350 μm . The furnace actual sensor reliability is $\pm 20K$. The full process can be resumed in the Fig. 1.

The samples stir for 5 minutes every 30 minutes in the furnace to ensure a better nickel adhesion (inlaid) on the B_4C surface. With graphite crucible and stick aiming to reduce the contamination. The reinforcement powders are analysed by laser scanning microscope (LSM), Raman spectroscopy (DRX), Infrared spectroscopy (FTIR) and X-ray powder diffraction (XRD).

On the second step, a SAA of 0.1 ml/g H_2SO_4 / B_4C (oxidized) is made. The H_2SO_4 self-decomposes in H_2O and HCl , the two main acids that strongly react with oxides and decompose ceramics [24]. The H_2SO_4 (99.00%) is carried out under chemical fume hood due to acid hazards with agitation for 10 minutes. The samples are then washed in abundance with hot water at 363K, filtered and dried at 373K for 60 minutes.

B. Semi-continuous casting and hot rolling

The Composite is produced by a simplified semi-continuous casting method and hot rolling. The outer layer of the composite is constituted by Al (99.70%). The AMC inner layer powder is constituted by Al (99.85%) and B_4C (as treated) powders in a ratio of 40wt.% (few samples with 10wt.% as treated/untreated and 40wt.% untreated are made to comparison). The powder is placed into a rotary drum mixer at 3.14 rad/s for 120 min. The casting method was designed based on previous work made by Xu *et al.* [1] as shown in Fig. 2. The mixed powders were placed in a stainless steel mould (dividing plate) supported by Al sheets (up and down sides). The molten Al (1023K) was poured into the stainless steel mould to form a solidified Al shell. During the casting process, the stainless steel dividing plate was elevated and the mixed powders gradually contacted with the liquid Al. After molten Al reaches the top of the mould, the composite is left to cool

down at room temperature ($\sim 288K$) and is then un moulded.

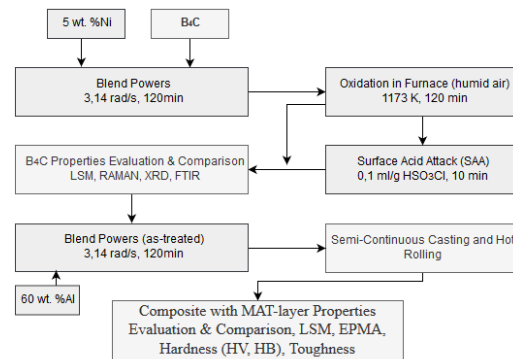


Fig.1 Composite acquisition diagram

After the casting process, the ingot is placed in an electric box resistance furnace at $723 \pm 10K$, this temperature improves the density of the composites and the bond between layers [25]. The rolling direction is unidirectional with the same direction of "Pull out direction" marked in Fig. 2. The hot rolling process reduces the cross section thickness from 75mm to 15mm, with 20 passes, it means a rolling reduction of 4% per pass, corresponding to a final reduction of 80%.

For microstructural examination, the composite samples were cut into small pieces (cross section 20 mm \times 15 mm) by line cutting, and then polished. To investigate the microstructure, a laser scanning microscope (LSM), an electron micro probe analyzer (EMPA) is used. The macro hardness test HBS1.5/125/30 was carried out at room temperature ($\sim 293K$) using a Digital Brinell Hardness Tester MHB-3000. The micro hardness test ISO 6507-1 (1Kg/15 seconds) is carried out in the Digital Vickers Hardness Tester machine. Impact toughness test samples were cut in 15x10 mm cross section with 100 mm length. The test was performed 3 times for each group along the transversal direction, the test energy was 150J.

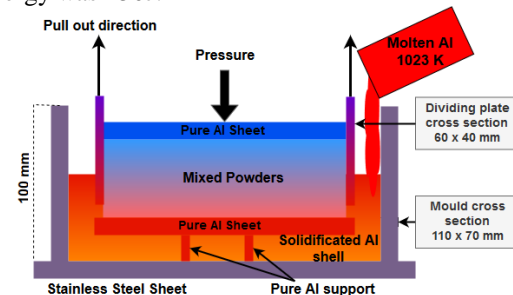


Fig.2 Semi-continuous casting method used to ingot acquisition

III. RESULTS AND DISCUSSION

A. Surface treatment

The B_4C oxidation must have a vitreous layer, thin and patchy at 973K thicker and continuous at 1073K-1173K continuous and with beading at 1273K-1473K. The B_4C reinforcement after the oxidation

shows strong color change and surface flaws reduction, such fact is explained by the oxide formation overlapping the entire reinforcement surface with a crystal-glass oxide layer. The main oxidation reaction produces B_2O_3 (glass/crystal) and CO_2 and secondary reactions in humid air also produce others boron and carbon compounds (H_3BO_3 , CO , etc.) [21]-[23].

The surface transformation is explained by Fig. 3, where (a) is the original B_4C surface, (b) is the B_4C -Ni(oxidized) reinforcement and (c) is the SSA given surface.

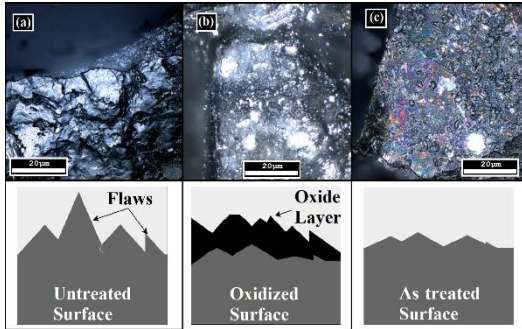


Fig. 3 Macrostructure of B_4C -5 wt.% Ni surfaces observed by LSM, (a) untreated, (b) Oxidized and (c) As treated surface

The Ni adhesion is observed by metallic color spots. In Fig.3(c) the principal flaws are not visible anymore and the whole surface is more “regular” and “flat” than the original surface present in Fig.3(a), some degree of “etching” also is observed. Such analysis demonstrates the oxide layer formed at this temperature and time is enough to oxidize the superficial imperfections and then the SAA is able to remove them in a macro scale [26]-[27].

The LSM only shows visually the reinforcement surface. To understand the compounds yielded and bounds in the reinforcement surface, the XRD is performed. The XRD patterns of the samples are given in Fig.4. Metallic Ni and borates seem to be the dominant phase in the oxidized sample. However, no catalyzing effect of Ni was observed at 1173K. Comparing the XRD (Fig. 4), the as treated and oxidized sample, some peaks attributed to B oxides as B_2O_3 are not present in SAA sample, meaning it has removed or it remains in an undetectable amount [28]-[31].

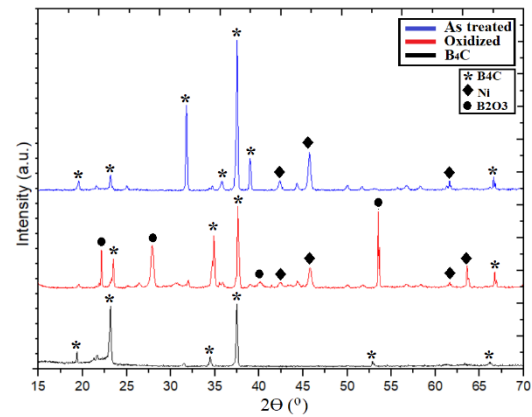


Fig.4 XRD patterns of B_4C -5 wt.% Ni for as treated, oxidized and untreated powder samples

In order to study clearly the bonds on reinforcement surface, the Raman and infrared analysis provide good information.

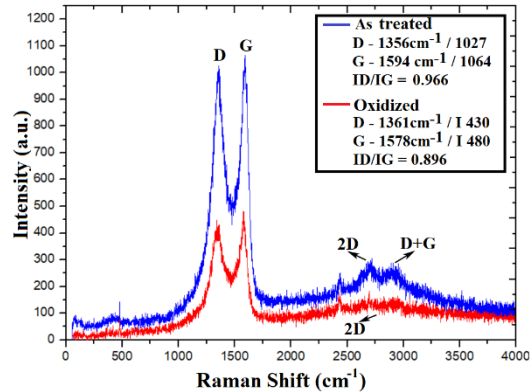


Fig. 5 Raman spectroscopy of B_4C -5 wt.% Ni for as treated and oxidized powder samples

The Raman spectroscopy (Fig. 5) shows a typical carbon D and G bands. The D and G bands intensity ratio put this carbon as a glassy or cluster carbon on the surface. The D band has a peak around 1350 cm^{-1} which is attributed to carbon sp^2 carbon bonds. The G band is not clear about its source and this issue generates a lot of discussion amongst researchers, having different attributions according to different references.

The peak around 1580 cm^{-1} does not seem to be a spectrum of boron carbide. This peak is present in the Raman spectra of carbon-rich boron carbides as well, and in this composition range the existence of free carbon in boron carbide may be excluded. This peak can be ascertained that at any carbon content in carbon-rich B_4C considerable concentration of C-B-B chains exists [32]-[34].

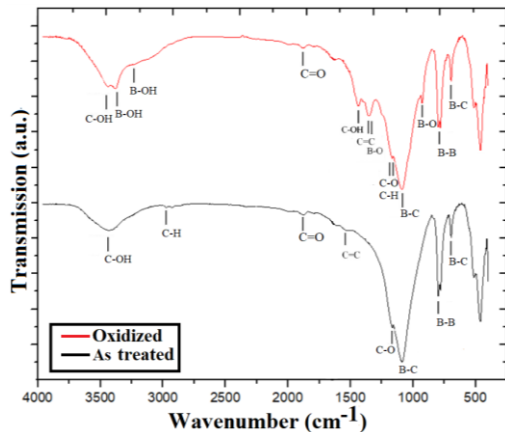


Fig. 6 FTIR of B_4C -5 wt.% Ni for oxidized and as treated powder samples

The FTIR of the oxidized powder bands shows elements around 3485cm^{-1} (C-OH), 3265cm^{-1} (B-OH), 1462cm^{-1} (B-OH), 1395cm^{-1} (C-OH), 1249cm^{-1} (B-O), 1188cm^{-1} (C-O) corresponded to boron carbon oxides. The result also confirms that boron oxide is mainly removed from the B_4C surface through SAA due to (B-O) bonds reduction. The band at 2368cm^{-1} ascribed to free carbon is not found in any analysis in accordance to the Raman analysis possible excluding the free carbon reposition [34].

The chemical bonding of the SAA B_4C powder that has a strongest vibration around 1079cm^{-1} (B-C) can be attributed to the characteristic intericosahedral B_4C vibration. The boron oxide in as treated powder probably originated from incomplete oxides removal or it is a contaminant. The peaks around 837cm^{-1} and 605cm^{-1} are also in agreement with the reported typical B_4C vibration band. The weak peak about 1188cm^{-1} should be assigned to (C-O). The broad band at 3485cm^{-1} was attributed to the (O-H) vibration. The peak around 2900cm^{-1} is ascribed to the (C-H) band, which may represent one contaminate.

The conclusion that can be abstracted from the XRD, Raman and FTIR analysis are; The boron oxides are mainly removed, but possibly have some residues. carbon oxides are probably in gas phase and released out to the atmosphere, but free carbon may be present in crystal-glassy phase. Ni is truly inlaid to the reinforcement surface and it has no catalyst effect, peradventure it can yield to some interactions with carbon, boron and oxygen, despite Ni bonds are not

in strong intensity in the analyses [35]. Some contaminations as water are present in as treated reinforcement. After those analysis, the reinforcement shows the desired properties; a regular surface with nickel inlaid, a surface with low oxides concentration and probably a surface with high carbon bounds disorder.

B. AMC Inner layer microstructure

The microstructure analysis of the composite inner layer shows a visible MAT layer boundaries the reinforcements as shown in Fig. 6(a) and 6(b) by different techniques. This layer is possibly composed of intermetallic particles as Ni_3Al , or Ni-Al rich particles dispensed an amorphous Al-Ni-C-B phase. This MAT layer boundary the reinforcement is responsible for reducing the residual stress, the properties gradient between the reinforcement/matrix and the interface line effect. There are some problems to analyse the over sized reinforcements with the traditional polish method, once it does not allow a flat polishing, being quite difficult to deeply understand the properties in the reinforcement and MAT layer interface. The elements concentration in the MAT layer is undefined and shows large range of different stoichiometry for each micro region, being it analysed by scanning or point EPMA stoichiometry. These layer thickness are not constant and can vary their characteristics from few micrometers to times larger than the bounded reinforcement. A mechanism to control such properties are not deeply studied in this work once it is not the main objective of it. Despite the difficulty to measure the amorphous layer composition, this layer's effect can be easily observed. Comparing Fig. 6(a) and (b), the big gradient properties lead to a bad composability and interface line formation between the reinforcement and matrix, such fact is demonstrated by the yellow arrow in Fig. 6(b) and Fig. 6(d). These distortions are not visible in Fig. 6(a) and Fig. 6(c) that has a MAT layer. The surface treatment also reduces reinforcement flaws as cracks present in Fig. 6(d) (blue arrow). For example, the micro particles and voids present in Fig. 6(d) were probably originated from previous microcracks present in the reinforcement surface. The origin of the crack and the void bounding the reinforcement will reduce the reinforcement effectiveness.

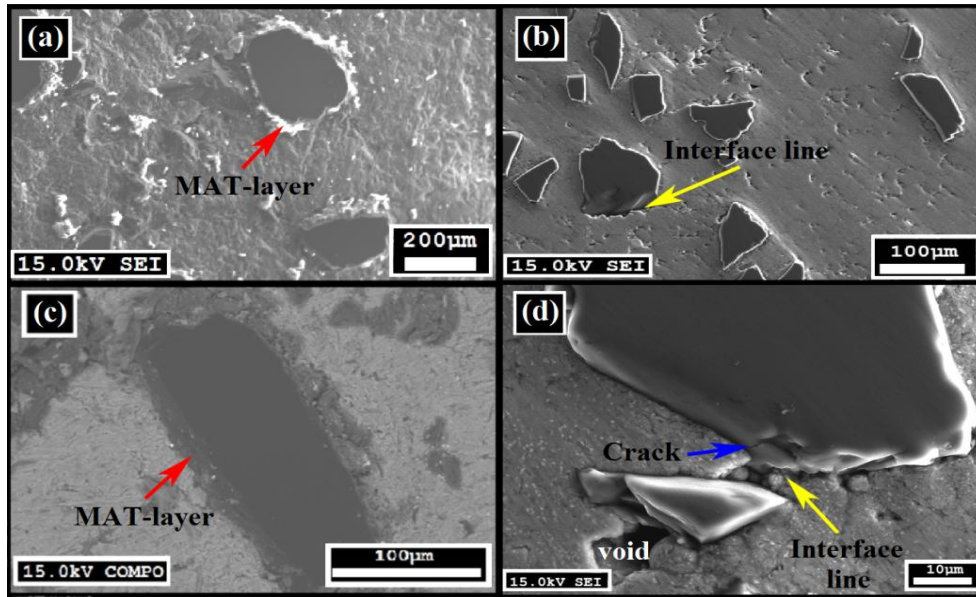


Fig. 6 Microstructure of the composite made by as treated powders in (a) and (c) with the MAT layer formation by different EPMA technics. Figures (b) and (d) are composites made by untreated powders. The yellow arrows are interface lines and blue arrow is a micro crack.

C. AMC Micro and Macro Properties

The micro hardness tested from a point on transition layer immediately after B₄C and MAT layer interface going towards the matrix shows some similarity with an exponential decay function Equation (1). This fact may demonstrate the correlation to bulk diffusion and MAT layer formation. Although it is related with diffusion, for amorphous materials, the stoichiometric formula is undefined and some constants on Arrhenius diffusion equation cannot be explicit. Based on the decay function, the following similarity can be made with the following conditions:

$$P_x = p_\infty + p_0 e^{-\delta x} \quad (1)$$

Where, P_x is a property (hardness, density, etc.), p_∞ is the matrix properties considering it is homogeneous, (r_0) is the average reinforcement radius (approaching it as circumferential), $P_0 = P(0)$ is the initial quantity at $x=r_0$, and δ is empirical value related to the decay rate. For such approximation to be valid some conditions must be taken; Assume the distance (x) is always greater than (r_0) . Experimentally for (x) greater than $10r_0$ the radius can be considered infinite and only the matrix properties take effect. This conclusion is shown in Fig. 7.

To manipulate the gradient intensity for the matrix micro hardness, the average distance between the reinforcements is needed and it can be found by the relation in equation (2) [1]. Using as input data only the volumetric fractions of each component and the reinforcement average radius, the prediction of the matrix average hardness is done when $x = \lambda$ is introduced in the Equation (1) from relation (2).

$$\lambda = \frac{4(1-f)r_0}{3f} \quad (2)$$

Where λ is the distance between the reinforcements, f is the reinforcement fractional volume. The experimental and calculated micro hardness data are plotted in Fig. 7 using empirical δ .

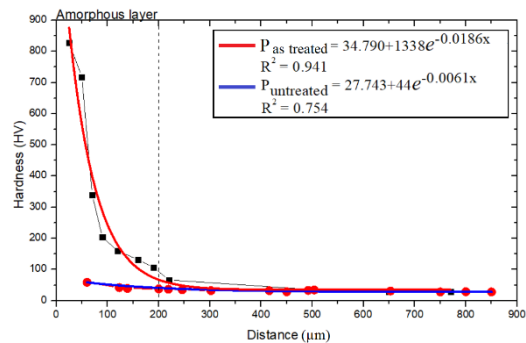


Fig. 7 The micro hardness test (HV) of composites made by as treated and untreated powders

To measure the macro theoretical properties, the following relation can be used [14].

$$E_c = E_m V_m + K_c E_r V_r \quad (3)$$

Where, K_c is an experimental constant between 0 and 1. This range of values for K_c reflects that the particle reinforced composites are not characterized by the iso-strain condition, E is the property to be evaluated, V is the mass fraction. The subscripts c, m, r refers to composite, matrix, and reinforcement, respectively. The Brinell hardness test is demonstrated in Fig. 8(a). The tested samples are demonstrated in Fig. 8(b).

The sample with 40 wt.% B₄C untreated demonstrates poor results cracking under the test load as show in Fig. 8(c). Admit the macro hardness as “ E ” property in the relation (3).

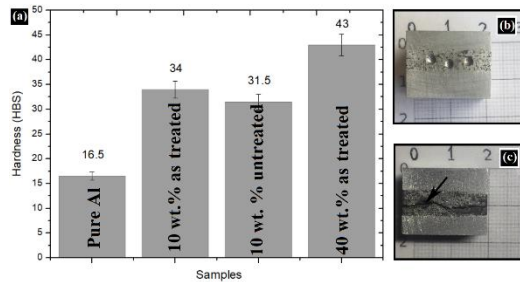


Fig. 8 The Brinell hardness test HBS1.5/125/30 of Al and composites made by untreated and astreated powder

Abstracting the data from the experimental plot (Fig. 8) it is possible to calculate the empirical values of K_c . To the sample 10wt.% B_4C untreated the K_c is 0.0710 and to 40wt.% as treated the K_c is 0.0344, it clearly shows the effect of adding large amounts of reinforcement modifies the final composite properties. Abstracting data from experiments made under similar circumstances (40wt.% B_4C main size $23\mu m$, without MAT layer) it demonstrates K_c equals to 0.03477, and for 40wt.% B_4C main size $70\mu m$ [1] the K_c is 0.0277. Assuming K_c linear the expected value to 60 mesh is 40% less than one with MAT layer.

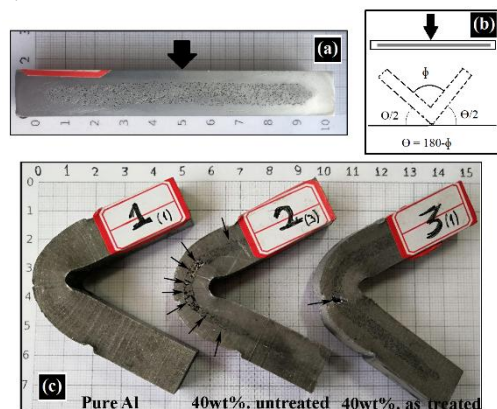


Fig. 9 Impact toughness response of Al and composites made by untreated and astreated powder

The problem in any composite with large relative reinforcements size are the defects as cracks on the interface making it very fragile, failing catastrophically under low load. Fig. 9 demonstrates the impact toughness test. The pure Al sample has an absence of fractures due to its own ductility. To the sample 40wt.% B_4C untreated, the brittle fracture in the innerlayer is quite visible showing the facility to the cracks propagation. To the last sample 40wt.% B_4C as treated, one macro crack is noted, and that crack leads the composite to failure. Despite the failure, the quantity of macro cracks is extremely lower than a same composite without surface treatment and MAT layer. One more way to quantify the difference between the composites is by analyzing the deformation angle ϕ formed after the

impact, once it has not cracked under test load. The tested samples angles are $\phi_1=57^\circ$, $\phi_2=56^\circ$ and $\phi_3=71^\circ$ ($\pm 5^\circ$), the bigger angle in the sample as treated shows the innerlayer contribution to the composite toughness. However the low value on the untreated samples almost the same as the pure aluminum expresses in this case the innerlayer does not have a significant influence due to composite toughness [36]-[37].

IV. CONCLUSION

The Al-Al+ B_4C -Al layered composites were produced by semi-continuous casting method and hot rolling, the microstructure and mechanical properties were evaluated. From the study, the following conclusions can be abstracted:

- The B_4C powders are successfully oxidized and the SAA removes surface oxides and imperfections.
- The MAT layer was formed and it is beneficial to the layered AMC mechanical properties.
- Improving the reinforcement surface and inserting a MAT layer raises the composite mechanical properties allowing the utilization of high reinforcement size and wt.% in composites innerlayer to engineering applications.

ACKNOWLEDGMENTS

This research was supported by a Dalian University of Technology, Laboratory of Special Processing of Raw Materials and School of Material Science and Engineering, Dalian University of Technology, Dalian, Liaoning 116024, China.

REFERENCES

- [1] G. Y. Xu, Y. H. Yu, Y. B. Zhang, T. J. Li, T. M. Wang, "Effect of B_4C particle size on the mechanical properties of B_4C reinforced aluminum matrix layered composite". *SECM*, v. 26, Issue 1, p. 53-61.
- [2] Y. Z. Li, Q. Z. Wang, W. G. Wang, B. L. Xiao, Z. Y. Ma, "Effect of interfacial reaction on age-hardening ability of $B_4C/6061Al$ composites", *Materials Science and Engineering A* 620, pp. 445-453.
- [3] Vikrant Chandel, Onkar Singh Bhatia "Fabrication and Characterization of Al 7075-Cenosphere Composite & its comparison with pure Al 7075", *International Journal of Engineering Trends and Technology (IJETT)*, V29(3), pp. 133-142 Nov. 2015.
- [4] Y. B. Zhang, Y. H. Yu, G. Y. Xu, Y. Fu, T. J. Li, T. G. Wang, Q. T. Guo, "Microstructure and Performance of a Three-Layered Al/7075- B_4C /Al Composite Prepared by Semi Continuous Casting and Hot Rolling", *Metallurgy Journal* 8(8):600. 2017.
- [5] F. Thévenot. "Boron Carbide A Comprehensive Review". *J. Eur. Ceram. Soc* 6, pp. 205-225, 1990.
- [6] N. K. Shrestha, M. Kawai, T. Saji. "Co-deposition of B_4C particles and nickel under the influence of a redox-active surfactant and anti-wear property of the coatings". *Surface & Coatings Tech.* pp.2414-2419, 2005.
- [7] A. Ektarawong, S. I. Simak, L. Hultman, J. Birch, B. Alling. "First-principles study of configurational disorder in B_4C using a superatom-special quasirandom structure method". *Physical Review B*, Vol. 90, Issue 2, July. 2014.
- [8] J. H. Wang, Y. He, Z. F. Xie, C. L. Chen, Q. B. Yang, C. L. Zhang, B. Y. Wang, Y. Q. Zhan, T. H. Zhao, "Functionalized boron carbide for enhancement of

- anticorrosion performance of epoxy resin”, *Polymers Adv. Technologies*, pp. 758-766, Feb. 2018.
- [9] I. Topcu, H.O. Gulsoy, N. Kadioglu, A.N. Gulluoglu. “Processing and mechanical properties of B4C reinforced Al matrix composites”. *Journal of Alloys and Compounds*, 482, pp. 516-521, 2009.
- [10] R. Telle. “Oxidation behavior of B4C-SiC composites with various microstructures”. *AIP Conference Proceedings*, 1991, 231, p. 553.
- [11] L. M. Litz, R. A. Mercuri. “Oxidation of Boron Carbide by Air, Water, and Air-Water Mixtures at Elevated Temperatures”. *Journal of The Electrochemical Society* 110(8), Jan. 1963.
- [12] D. M. Bylander, L. Kleinman, S. B. Lee. Self-consistent calculations of the energy bands and bonding properties of $B_{12}C_3$. *Phys. Rev. B* 42, 1990.
- [13] E. Ghasali, M. Alizadeh, T. Ebadzadeh, A.H. Pakseresht, A. Rahbari. Investigation on microstructural and mechanical properties of B4C-aluminum matrix composites prepared by microwave sintering. *J Mater Res Technol*;4(4), p. 411-415, 2015.
- [14] H. Courtney, Thomas. *Mechanical behavior of materials*. 2nd ed, Boston: McGraw Hill. 2000.
- [15] D. M. Scruggs, “Composite material bonded by an amorphous metal, and preparation thereof”, United States patent, US4621031A, August, 01, 1994.
- [16] L. F. Bailey, R. J. Bennett, “DICOR® Surface Treatments for Enhanced Bonding”, *Journal of Dental Research* 67(6), p. 925-3, Jul, 1988.
- [17] V. A. Lavrenko, A. P. Pomytkin, P. S. Kislyj, B. L. Grabchuk, “Kinetics of High-Temperature Oxidation of Boron Carbide in Oxygen”, *Oxidation of Metals*, Vol. 10, No. 2, 1976.
- [18] C.W. San Marchi. “Processing of Aluminum-Nickel Amorphous by Reactive Infiltration”, PHD Eng. thesis, MIT, USA, 1997.
- [19] (2018) AZoN, Scientists Develop Nickel Aluminide Composite Material that Can Cut Through Cast Iron and Granite, [Online]. Available: <https://www.azom.com/news.aspx?newsID=3866>
- [20] B. K. Ozcelik, C. Ergun, “Effect of Ni on The Synthesize Boron Carbide Via Aerosol Method”, *Researchgate*. RG.2.1.4392.1765, July 2015.
- [21] H. Shmue. “Reaction-bonded boron carbide for lightweight armor: The interrelationship between processing, microstructure, and mechanical properties”, *American Ceramic Society Bulletin*, Vol. 96, No. 6 pp. 20-26, August 2007.
- [22] A. Kilicarslan, F. Toptan, I. Kerti, S. Piskin, “Oxidation of boron carbide particles at low temperatures”, *Mat. Letters*, 128(1), pp. 224-226, 2014.
- [23] Y.Q. Li, T. Qiu, “Oxidation behaviour of boron carbide powder”, *Materials Science and Engineering A* 444, pp. 184-191, 2007.
- [24] (2018) NIH U.S. Compound Summary for CID 24638. Chlorosulfonic acid. [Online] available : https://pubchem.ncbi.nlm.nih.gov/compound/Chlorosulfuric_acid#section=Top.
- [25] Redankamma Yenumula, Srinivasulu Dorasila, CV Ramana Murthy Naidu S, Rambabu Kalpukuri, "Experimental Investigation of Mechanical Properties of Pure Al-Sic Metal Matrix Composite by Stir Casting Method", *International Journal of Engineering Trends and Technology (IJETT)*, V59(3), 148-154 May 2018.
- [26] M. Kern, Vol. P. Thompson, “Bonding to glass infiltrated alumina ceramic: Adhesive methods and their durability”, *The Journal of Prosthetic Dentistry*, 73(3):240-9, Mar, 2005.
- [27] Y. Chaiyabutr, S. McGowan, K. M. Phillips, J. C. Kois, R. A. Giordano, “The effect of hydrofluoric acid surface treatment and bond strength of a zirconia veneering ceramic”, *The Journal of Prosthetic Dentistry* Vol. 100, Issue 3, Sept. 2008, p. 194-202.
- [28] Mike Glazer, *International Tables for Crystallography*. International Union of Crystallography, Vol. A, ch. 2.3, pp. 193-687, 2006.
- [29] J. A. Bigdeloo, And A. M. Hadian, “Synthesis of High Purity Micron Size Boron Carbide Powder from B2O3/C Precursor”, *International Journal of Recent Trends in Engineering*, Vol. 1, No. 5, May 2009.
- [30] I.A. Rakhmatullin, A.A. Sivkov, A.F. Makarova, “Boron carbide nanopowder synthesized using electrical discharge plasma”, *Journal of Physics, Conference Series* 552, 012008, 2014.
- [31] H. Saitoh, K. Yoshida, W. A. Yarbrougha. “Crystal structure of new composition boron-rich boron nitride using Raman spectroscopy”. *J. Mater. Res.*, Vol. 8, No. 1, Jan 1993.
- [32] D. R. Tallant, T. L. Aselage, A. N. Campbell, and D. Emin. “Boron carbide structure by Raman spectroscopy”, *Phys. Rev. B* 40, p. 5649, 1989.
- [33] D. R. Tallant, T. L. Aselage, and D. Emin, “Structure of icosahedral borides by Raman spectroscopy”, *AIP Conference Proceedings* 231, p. 301, 1991.
- [34] K. I. Sasaki, Y. Tokura, T. Sogawa. “The Origin of Raman D Band: Bonding and Antibonding Orbitals in Graphene”, *Crystals*, Vol. 3, pp. 120-140, 2013.
- [35] F. Davar, Z. Fereshteh, M. Salavati-Niasari, “Nanoparticles Ni and NiO: Synthesis, characterization and magnetic properties”, *Journal of Alloys and Compounds* 476, pp. 797-801, 2009.
- [36] B. Raj, K. Bhanu, S. Rao, *Mechanical Testing: Overview*, *Encyclopedia of Materials: Science and Technology*, 2001.
- [37] F. Ouchterlony, *Fracture Toughness Testing of Rock*. Rossmannith, H.P. (eds) *Rock Fracture Mechanics*. International Centre for Mechanical Sciences, Vol. 275, Springer, Vienna, 1983.